crystals

MDPI

Article

Designing Continuous Crystallization Protocols for Curcumin Using PAT Obtained Batch Kinetics

Mayank Vashishtha [1,†], Mahmoud Ranjbar [1,†], Gavin Walker [1] and K. Vasanth Kumar [1,2,*]

[1] Department of Chemical Sciences, Synthesis and Solid State Pharmaceutical Research Centre, Bernal Research Institute, University of Limerick, V94 T9PX Limerick, Ireland
[2] Department of Chemical and Process Engineering, School of Chemistry and Chemical Engineering, Faculty of Engineering and Physical Sciences, University of Surrey, Guildford GU2 7XH, UK
* Correspondence: v.kannuchamy@surrey.ac.uk
† These authors contributed equally to this work.

Abstract: Developing theory-informed standard operating procedures (SOPs) for the continuous crystallisation of pharmaceuticals still remains a bottleneck. For the continuous manufacturing of pharmaceuticals, the current methods rely on the laborious trial-and-error approach to identify process conditions such as the dilution rate (flow per unit volume of reactor) and initial supersaturation, where the productivity will be at maximum at steady-state conditions. This approach, while proven and considered to be useful, lacks or ignores the information obtained from batch kinetics. Herein for the first time, we propose a theoretical method to develop batch kinetics-informed theoretical procedures for the continuous manufacturing of a model compound curcumin in isopropanol. The theoretical approach uses batch kinetic constants to theoretically identify the optimum dilution rate and the corresponding mass of the model compound curcumin when crystallised, as well as its productivity at steady-state conditions as a function of initial supersaturation. The theory-informed procedures will serve as a valuable guideline to develop operating procedures for the continuous production of the target compound and thus eliminate the trial-and-error approach used to develop the protocols for the continuous manufacturing of pharmaceuticals. We also showed that our methods allow for the estimation of the dilution rate that corresponds to washout conditions (i.e., where all the crystals in the crystalliser will be washed out due to the high flow rate of the input stream) during the continuous manufacturing of crystals.

Keywords: crystallization; batch kinetics; continuous crystallization; theory

check for updates

Citation: Vashishtha, M.; Ranjbar, M.; Walker, G.; Kumar, K.V. Designing Continuous Crystallization Protocols for Curcumin Using PAT Obtained Batch Kinetics. *Crystals* **2024**, *14*, 1069. https://doi.org/10.3390/cryst14121069

Academic Editor: Borislav Angelov

Received: 27 November 2024
Revised: 10 December 2024
Accepted: 10 December 2024
Published: 12 December 2024

Copyright: © 2024 by the authors. Licensee MDPI, Basel, Switzerland. This article is an open access article distributed under the terms and conditions of the Creative Commons Attribution (CC BY) license (https://creativecommons.org/licenses/by/4.0/).

1. Introduction

Crystallisation is an important separation and purification technique. Pharmaceutical industries use crystallisation to purify and isolate active pharmaceutical ingredients (APIs) in solid and crystalline forms [1–4]. After crystallisation, the purified APIs are transferred to other locations for temporary storage before undergoing a series of downstream unit operations to create oral drug dosage forms [5,6]. However, these downstream operations often occur in separate rooms or sites, necessitating the storage and transportation of APIs between locations. This process incurs high-energy consumption, manufacturing costs, and risks of product loss and contamination during transportation and storage [7]. Moreover, most pharmaceutical industries conduct both crystallisation and downstream operations in batch mode, leading to downtime [8–11]. To ensure regulatory compliance, particularly with FDA standards such as CGMP (Current Good Manufacturing Practice) and QbD (Quality by Design), each batch's product quality undergoes rigorous testing to detect and prevent batch-to-batch variations [12–14]. Failure to comply can result in costly recalls, contributing to the estimated $50 billion annual losses in the pharmaceutical industry due to inefficient manufacturing [15]. To address these challenges associated with the current state-of-the-art methods of batch manufacturing of APIs, there is a growing emphasis on

continuous manufacturing methods, advocated by the FDA, to enhance product quality, mitigate medicine shortages, and streamline regulatory compliance. This approach aims to create an uninterrupted production chain from raw materials to finished products, thereby improving efficiency and reducing manufacturing lead times [16]. However, many pharmaceutical facilities still predominantly operate on a batch crystallisation basis, leading to operational downtimes and regulatory challenges, notably from the US Food and Drug Administration (FDA) [6]. However, despite these advantages, many pharmaceutical industries still rely on batch processing due to challenges in integrating upstream crystallisation with downstream operations. One of the biggest challenges faced by both industries and crystallisation scientists is the lack of a unique method that allows them to develop a set of operating procedures for designing and operating a continuous crystallisation unit based on data from batch processes. Traditionally, or as a matter of practice or convenience, researchers have conducted crystallisation experiments in either batch or continuous mode, often treating these as separate and isolated processes. Furthermore, there has been a disconnect and lack of information exchange between the studies performed in batch and continuous mode. This limits the idea of using batch crystallisation kinetics as a guide to develop SOPs for continuous crystallisation. This lack of guidance from batch processes necessitates laborious trial experiments by process engineers to optimise conditions for continuous API production. Currently, the continuous manufacturing of APIs is often performed using a continuous stirred-tank reactor, often referred to as MSMPR (mixed-suspension mixed-product removal) in crystallisation literature [17–21]. The operating procedures or the protocols for continuous manufacturing in MSMPR are often developed using laborious multiple trial-and-error experiments. These trial-and-error experiments focus on identifying the process conditions required for manufacturing APIs in continuous mode [22–24]. The trial-and-error approach is issued to identify the dilution rate, which is defined as the flow rate per unit volume, and the degree of supercooling that ensures maximum productivity (defined as the mass produced per unit volume per unit of time) and products with a desired level of purity at steady-state conditions [25,26]. It is worth mentioning here that these approaches are empirical and rely on the experimental outcome of each experiment performed on a trial-and-error basis and do not rely on information obtained from batch kinetics. It will be advantageous to develop a theory and batch kinetics-informed procedures that eliminate the requirement to perform multiple trial experiments to develop operating procedures for the manufacturing of pharmaceuticals in a continuous model.

It should be acknowledged that batch crystallisation kinetics can be easily obtained from carefully designed experiments in batch mode. Multiple experiments at different scales are also easier to perform in batch mode, provided there is information about the solubility and metastable zone width of the targeted compound in a suitable solvent. There is a crucial need to develop a method that can exploit the readily obtained batch crystallisation kinetics and transpose this information to identify the process conditions required to produce a specific product with the desired level of productivity in a continuous mode.

In this work, we developed one such method to transpose the batch kinetics into procedures required to manufacture a model pharmaceutical compound in batch mode. We performed cooling crystallisation experiments in batch mode to obtain the crystallisation kinetics of curcumin as a function of initial supersaturation or the degree of supercooling. We used a first-order kinetic model to obtain the crystallisation kinetic constant that corresponds to conditions where the crystallisation rate is at maximum. Using this kinetic constant obtained solely from batch crystallisation kinetics, we developed a theoretical design procedure that relies on simple mass balance and first-order kinetics for the continuous manufacturing of curcumin in isopropanol for various dilution rates and degrees of supercooling. Curcumin is often manufactured using batch crystallisation approaches. In this work, we developed a theoretical protocol for the continuous crystallisation of this compound [27–32]. Our theoretical method allows us to calculate the productivity as a function of initial supersaturation or the degree of supercooling and dilution rate. Further-

more, irrespective of the initial supersaturation, using the theoretical method we proposed, we exploited batch kinetics to identify the required dilution rate to achieve maximum productivity and to identify the dilution rate that corresponds to washout conditions (where all the crystals will be washed out of the crystalliser leaving only the mother liquor in the crystalliser). The theoretical procedures developed in this work will serve as a guideline for crystallisation scientists aiming to develop continuous manufacturing processes for a targeted compound, provided they have already obtained the batch kinetics of the same compound in a suitable solvent.

2. Theory

Typically, continuous crystallisation is conducted within a stirred-tank crystalliser, often referred to as CSTC or MSMPR. Within this setup, the reactor houses a suspension wherein a continuously supplied supersaturated solution generates crystals while the depleted supersaturation feed is continuously extracted from the suspension. The suspension within the CSTC is thoroughly mixed, ensuring that the concentration of solids and supersaturation remains consistent throughout the crystalliser. Moreover, the suspension density within the CSTC and the effluent stream exiting the CSTC under steady-state conditions remain uniform. The CSTC can operate in two modes: *turbidostat* and *superstat*. In *turbidostat* mode, the feed flow rate is adjusted to maintain a constant suspension density. Many trial-and-error procedures developed in research laboratories aim to operate the CSTC in *turbidostat* mode, necessitating multiple experiments to identify optimal conditions [33]. Alternatively, in *superstat* mode, the feed conditions (supersaturation, feed flow rate) are held constant, allowing the system to attain a steady state. As shown later (in Section 4.1), the crystallisation of the model compound curcumin in isopropanol proceeds via at least four different kinetic regimes that include a lag phase, an exponential phase, and deceleration, followed by saturation. As we show later (in Section 4.1), kinetics are slower in the lag and deceleration phases when compared to the exponential phase. The mass crystallised increases exponentially with temperature, and the corresponding crystallisation rate will be higher when compared to the rate of crystallisation in the other three kinetic regimes. In the saturation phase, obviously there is no change in the solid-phase concentration, as the system has already reached saturation. It is important to operate the CSTC where the crystallisation rate is at maximum, which is in the exponential phase. This is a process analogue of a continuous stirred-tank fermenter operating in a *chemostat* mode [34]. In our work, we called it a crystalliser operating in a *superstat* mode. The intention here is to operate CSTC in *superstat* mode to eliminate the need of a trial-and-error approach while developing a theoretical operating procedure for the continuous crystallisation of curcumin. This means we need to identify the flow rate or the dilution rate (flow rate per unit volume per unit time) of the CSTC where the crystallisation rate will be at maximum. We will develop the theory below assuming that the CSTC is operated in such a way that the crystallisation rate in the crystalliser will be equal to the rate that corresponds to the exponential kinetic regime in the batch crystalliser. Based on this assumption, we propose a theoretical method to identify mathematically the dilution rate where the CSTC will be operating at conditions where the crystallisation rate will be in the exponential phase. The method also allows us to identify the dilution rate where the productivity (i.e., mass crystallised per unit volume and unit time) will be at maximum at steady-state conditions.

For a CSTC with a volume V (L), feed flow rate F (L/min), initial supersaturation ratio S_o, and solid concentration m_o (g/L), a material balance can be established over the CSTC using the following equation:

(Flow of material in) + (Formation of solids via crystallisation) − (Flow of material out) = Accumulation

For the mass crystallised, this becomes

$$F \cdot m_o + r_m V = Fm + \frac{dm}{dt} \cdot V \quad (1)$$

where r_m is the rate of crystallisation and this corresponds to the rate of formation of crystals per unit volume of the crystalliser per unit time.

At steady state, the change in solid concentration due to crystallisation in the solution becomes zero. Therefore, Equation (1) simplifies to

$$\frac{F}{V}(m_o - m) = D(m_o - m) = (-r_m) \tag{2}$$

where D denotes the dilution rate, which should be equal to the throughput rate.

If the rate of crystallisation, $-r_m$ (g/L·min), follows the first-order kinetics, it can be expressed as follows:

$$r_m = \frac{dm}{dt} = k{\cdot}m \tag{3}$$

We assume that the rate of change in the mass with respect to time due to crystallisation follows Equation (3), as this expression can well represent the crystallisation kinetics observed when the crystallisation is in the exponential phase (discussed later in Section 4.1). Equation (3) can be integrated with respect to the limits, $m = m_{o,}$ when $t = 0$ and $m = m$ when $t = t$. This should give a linear relationship: ln $(m/m_o) = kt$. In other words, according to Equation (3), theoretically, the plot of ln (m/m_o) versus t should be linear.

Substituting Equation (3) into Equation (2), we obtain the following:

$$D(m_o - m) = -k{\cdot}m \tag{4}$$

If the feed contains no crystals initially ($m_o = 0$), then Equation (4) simplifies to

$$D = k \tag{5}$$

Equation (5) essentially indicates the expected crystallisation rate in the solution as a function of the dilution rate. It is feasible to demonstrate that within a specific range of supersaturation, the kinetic constant k varies with supersaturation according to the following relation:

$$k = A(S_o)^n \tag{6}$$

Equation (6) can be substituted in Equation (4) as follows:

$$D(m_o - m) = -A(S_o)^n m \tag{7}$$

For crystallisation, the mass crystallised correlates directly with the depletion in supersaturation. The amount of mass crystallised in a solution is equal to the mass of the crystallising compound depleted in that solution. Thus, it is possible to define a parameter called the crystallisation coefficient, denoted as Y, which is the ratio of the depletion in supersaturation to the mass crystallised:

$$Y = \frac{S_o - S}{m - m_o} \tag{8}$$

where S and m are the supersaturation and the mass crystallised at any time, respectively. In this work, supersaturation is defined in terms of the supersaturation ratio c/c^*. S_o is the initial supersaturation and m_o is the mass of the crystal in the crystalliser when time $t = 0$. For the case of crystallisation at a fixed temperature, the value of Y will be unique. This can be typically obtained from the plot of S versus m. The value of S as a function of m can be calculated based on the solubility of the crystallising compound at the studied temperature T. In this work, we used curcumin as a model compound and isopropanol as a model solvent, and we studied the crystallisation at a temperature of $T = 5$ °C. At $T = 5$ °C, the solubility of curcumin in isopropanol is 0.76 g/L. For this combination of API and solvent, the $1/Y$ value was found to be equal to 0.76. It is important to note that this

value may vary with temperature but remains independent of the supersaturation S at a constant temperature T.

Equations (6)–(8) can be utilised to derive the concentration of solids in the CSTC at steady state, expressed as follows:

$$m = m_o + \frac{\left(S_o - \left(\frac{D}{a}\right)^{\left(\frac{1}{n}\right)}\right)}{Y} \quad (9)$$

Given the mass crystallised under steady-state conditions, we can define productivity as the mass crystallised per unit volume per unit time. This can be calculated by multiplying the dilution rate by the mass crystallised per unit volume of the reactor. Thus, productivity P can be determined as follows:

$$P = Dm = D{\cdot}m_o + \frac{DS_o}{Y} - \frac{D\left(\frac{D}{a}\right)^{\frac{1}{n}}}{Y} \quad (10)$$

Equation (10) enables the calculation of productivity in a *superstat* at varying dilution rates and supersaturation levels, provided that the kinetic information obtained from batch kinetics is available (note that the kinetic constant k is related to the constants a and $1/n$ in Equation (10).

3. Experimental

3.1. Materials

Crude CUR, obtained from Merck (Darmsta dt, Germany) (CAS. Reg. No. 458-37-7) with a nominal purity exceeding 75%, contains less than 5 wt% BDMC and less than 20 wt% DMC. HPLC-grade IPA, with a purity exceeding 99.9%, was purchased from Sigma Aldrich (CAS. Reg. No. 67-63-0). Our own laboratory HPLC analysis indicated that the curcumin is 78.6% pure, with less than 18 wt% DMC and less than 4 wt% BDMC. Curcumin was used as received for all the crystallisation experiments [31].

3.2. Crystal Growth Experiments

Cooling crystallisation experiments were conducted in batch mode utilizing a 100 mL Mettler Toledo's EasyMax 102 workstation (Mettler Toledo, Leicester, UK) with a reactor volume of 100 mL. Temperature control within the crystalliser was achieved through an external jacket employing electrical heating and solid-state cooling technology. Agitation throughout all experiments was maintained at 250 rpm using an overhead stirrer. Suspension density was monitored during the crystallisation process using in situ Raman spectroscopy. Crystallisation experiments were performed by adding a known mass of crude curcumin to 78.6 g of isopropanol. Heating the solution to 75 °C at a rapid rate ensured the dissolution of all solids. Subsequently, the solution was held at 75 °C for 45 min to guarantee complete dissolution of the curcumin. Supersaturation was achieved by cooling the solution to the working temperature of 3 °C at a rate of 8 K/min. Once the solution reached the working temperature, we added 0.0416 g of seed crystals to trigger the secondary nucleation. This amount is equal to a seed loading of 2.76 to 1.23 wt% depending on the initial supersaturation. In this work, we performed crystallisation experiments with solutions of five different initial supersaturations, S_o = 3, 3.5, 4, 4.5, 5, and 5.5. Supersaturation is defined here in terms of the supersaturation ratio given by c/c^*, where c is the concentration of the solution and c^* is the solubility concentration at the working temperature. The solubility concentration was obtained from the literature; at 3 °C, the solubility of curcumin in isopropanol is equal to 0.76 g/L. After adding the seeds, we maintained the working temperature for approximately 24 h to achieve complete saturation. The seeds are added intentionally to trigger secondary nucleation. Each experiment was conducted based on the procedures mentioned above. The experimental procedure was created as a recipe and executed using Mettler Toledo's iControl software v4.3.

Throughout the course of the crystallisation experiments, we monitored the suspension density using the in situ Raman spectroscopy (Kaiser Optical System, Inc. RX1 Raman, Ann Arbor, MI, USA). The Raman intensity was then converted into suspension density expressed in terms of mass crystallised per unit volume using a two-point calibration-free method proposed in our earlier works [1,2].

3.3. Seed Crystals

Seed crystals used in the crystallisation experiments were prepared via primary nucleation at a working temperature of 5 °C and at a fixed agitation speed of 250 RPM. For this, we added 0.6 g of crude curcumin in isopropanol solution. The solution was then heated to 75 °C and we maintained the solution at this temperature for 45 min to ensure complete dissolution of the crystals. Then, we cooled the solution to the working temperature of 5 °C at a rate of 8 K/min. Once the solution reached the working temperature, we maintained the solution temperature at this temperature for 24 h, which is sufficient to observe primary nucleation followed by growth until the solution reaches the solubility limit. After 24 h, we filtered the crystals via a vacuum filtration technique, and we dried the crystals in a fume hood at room temperature in the absence of light.

4. Results and Discussions

4.1. Batch Crystallisation Kinetics

In Figure 1a, we show the plot of mass of curcumin crystallised in a batch reactor versus time at different initial supersaturations. Irrespective of the initial supersaturation, we observed four distinct kinetic regimes. For convenience, we show the different kinetic regimes separately in Figure 1b for the data obtained from a solution of initial supersaturation at $S_o = 3$. From Figure 1b, it can be observed that there exists a slight lag during the initial phase, followed by a rapid increase in the mass crystallised followed by slow kinetics, and finally the solution reaches a plateau when the solution concentration reaches the solubility limit. From the plot, it is reasonable to assume that the crystallisation rate is high in the region where we observe a linear and rapid increase of crystallised mass with respect to the time. We presume the crystallisation kinetics in this region are dictated by the combination of secondary nucleation and crystal growth. We obtain the rate kinetic constant for the crystallisation from this region using Equation (3). This kinetic constant obtained from this linear region, assuming the crystallisation kinetics follow the first-order kinetics and further assuming the crystallisation rate in this regime is constant and at maximum supersaturation, $S = S_o$. According to the first-order kinetics (or Equation (3)), the plot of ln (m/m_o) versus time should be linear. In Figure 1c, we plotted the ln (m/m_o) versus t for differences in initial supersaturation, S_o. It is evident from Figure 1c that there exists a linear relationship between ln (m/m_o) and t. The coefficient of determination (R^2) between the experimental data and the predictions from the linearised form of Equation (3) consistently exceeds 0.90. This strong correlation indicates that crystallisation during the exponential phase adheres to the first-order kinetic expression described by Equation (3).

In terms of the effect of initial supersaturation, it is evident from Figure 1a that the mass crystallisation rate increases with S_o. This trend is expected, as the driving force required for crystallisation increases with S_o, and this should increase the crystallisation rate. It is worth mentioning that while the observed noise in the PAT data (Figure 1a) could be reduced using a moving average method (e.g., averaging each point over 50 data points), this procedure is not essential for our objective of developing a theory from batch kinetics-informed design protocols for continuous crystallisation. The simplest first-order model fitted to the original PAT data is sufficient enough to effectively capture the experimentally observed trends (between the mass crystallised and time as a function of S_o) within the kinetic regime of interest without additional data smoothing.

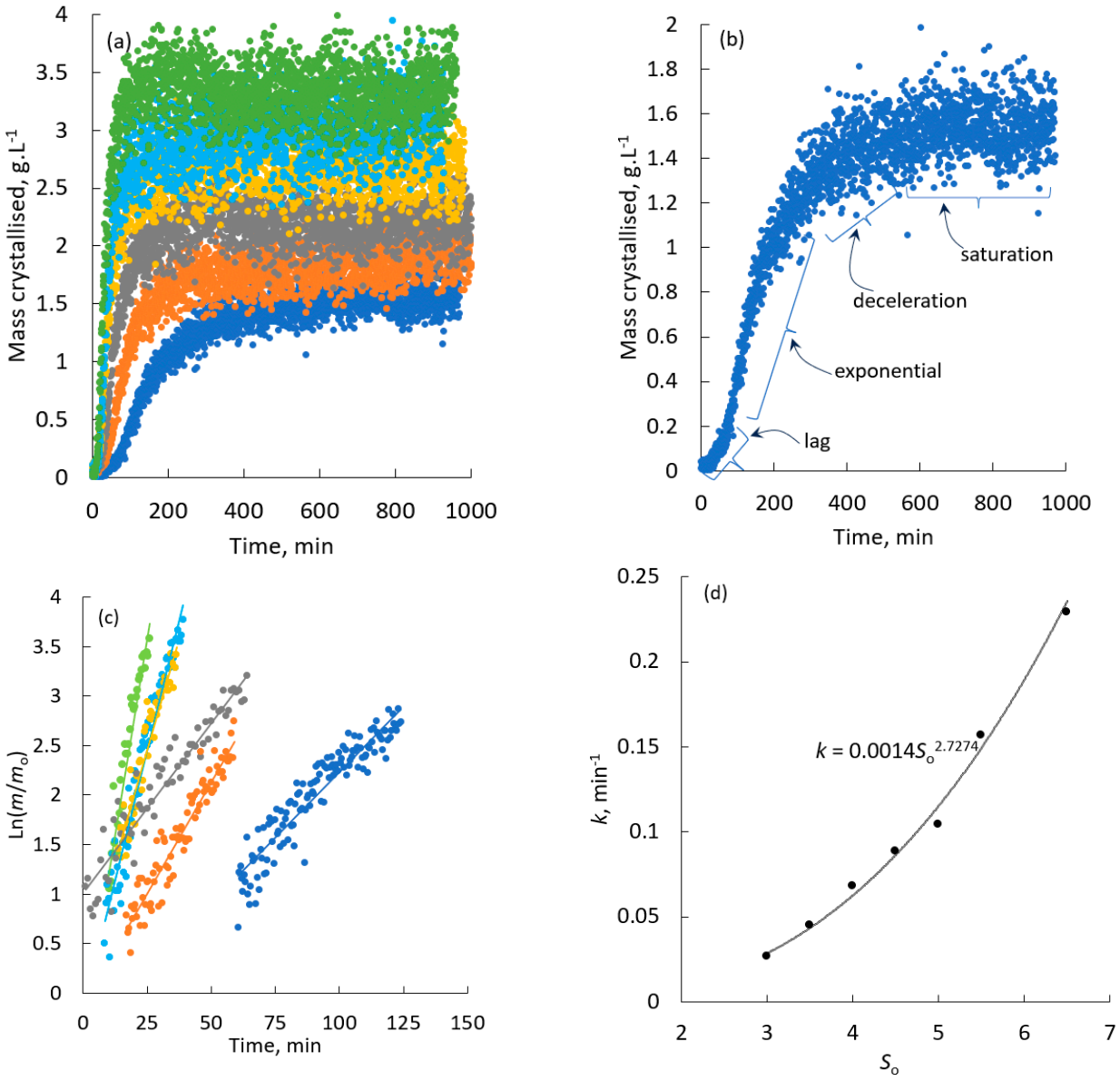


Figure 1. (**a**) plot of mass crystallised versus time (●: S_o = 3, ●: S_o = 3.5, ●: S_o = 4, ●: 4.5, ●: S_o = 5, ●: S_o = 5.5). (**b**) shows the different kinetic regimes involved in the crystallisation process (●: S_o = 3), (**c**) plot of ln (m/m_o) versus t (●: S_o = 3, ●: S_o = 3.5, ●: S_o = 4, ●: 4.5, ●: S_o = 5, ●: S_o = 5.5), and (**d**) plot of the kinetic constant, k, versus initial supersaturation.

The crystallisation kinetic constant, k, was obtained from the slope of this plot according to Equation (3). In Figure 1d, we plotted the kinetic constant k as a function of S_o. It can be realised from the figure that there exists a power law type of relation between k and S, given by the following:

$$k = 0.0044 S_o^{\ 2.7274} \quad (11)$$

Using the k values obtained using Equation (11) and the Equations (7), (9), and (10), we obtained both the mass crystallised and productivity at steady state as a function of the dilution rate for different initial supersaturations, and the results are discussed in the next section.

4.2. Continuous Crystallisation of Curcumin: Theoretical Prediction

Based on the batch kinetics discussed in the previous section and using the determined kinetic constants, it is possible to design an experimental protocol for the continuous crys-

tallisation of curcumin. For this, first we assume that the CSTC is operated in a *superstat* mode. This means we will fix the feed supersaturation and will operate the CSTC at a dilution rate where the crystallisation rate can be expected to be in the exponential regime (see Figure 1b). Once the initial supersaturation is fixed, it is possible to theoretically calculate the expected concentration of the solids in the crystalliser at the steady state. If the crystallisation rate within the CSTC is in the exponential phase, then the corresponding kinetic constant can be obtained from the batch kinetics as a function of feed supersaturation, and this should be theoretically equal to k. Using the kinetic constant k, we can theoretically predict the mass crystallised and the productivity at steady state using Equation (9) and Equation (10), respectively (see Section 2). The plot of mass crystallised at steady state (obtained using Equation (9)) versus dilution rate and productivity (obtained using Equation (10)) versus dilution rate for different initial supersaturations are shown in Figure 2a,b, respectively. Note that we used dilution rate (D) instead of defining a suitable flow rate (F) or defining a specific reactor volume (V) for theoretical convenience. Dilution rate, $D = F/V$. incorporates both parameters and thus, if we fixed the reactor volume, then from dilution rate we can predict the feed flow rate F that ensures a targeted theoretical mass that can be crystallised or the productivity. From Figure 2a,b, it can be observed that irrespective of the initial supersaturation, the theoretical mass crystallised at steady state decreases exponentially with an increase in the dilution rate. The higher the initial supersaturation, the observed exponential decrease with dilution rate is slower. In terms of productivity, it increases with an increase in dilution rate reaching a maximum followed by an exponential decrease with the dilution rate. There exists an optimum productivity, and this occurs when the productivity reaches the optimum dilution rate, D_{opt}. We also noticed that the mass crystallised and the productivity reaches zero at higher dilution rates in solutions with lower initial supersaturations. Clearly, productivity strongly depends on the initial supersaturation. For instance, the productivity reached zero when $D = 0.0445$ min^{-1} for $S_o = 3.5$. This corresponds to the conditions when all the crystals in the CSTC are washed out or conditions where we can observe no crystallisation via secondary nucleation or growth. However, when $S_o = 5$, we observed productivity closer to the maximum at the same dilution rate of 0.0445 min^{-1}. This clearly exposes the importance of the dilution rate on productivity and on the observed theoretical condition where productivity is zero. The zero productivity for higher dilution rates in solutions with lower supersaturations should be due to the fact that the supersaturation was diluted enough to observe no secondary nucleation, rather than solely due to the washout of the crystals (if any) in the CSTC. The optimum dilution rates for S_o seem to match with the ones obtained using Equation (12):

$$D_{opt} = a\left(\frac{(nY)(m_oY + S_o}{(n+1)Y}\right)^n \tag{12}$$

To derive Equation (12), we start by differentiating Equation (9) with respect to the dilution rate (D) and then set the result to zero, indicating that the productivity (P) is maximised at the optimal dilution rate (D_{opt}).

This can be expressed as $dP/dD = 0$. Next, we substitute $D = D_{opt}$ into the resulting expression. Another important observation is that D_{opt} is constant, but it depends on the initial supersaturation. Likewise, the mass crystallised and the productivity, when the $D = D_{opt}$ can be theoretically calculated by substituting Equation (12) in Equations (9) and (10), is as follows:

$$m_{opt} = m_o + \frac{\left(S_o - \left(\frac{D_{opt}}{a}\right)^{\left(\frac{1}{n}\right)}\right)}{Y} \tag{13}$$

$$P_{opt} = D_{opt}m_{opt} = D_{opt}m_o + \frac{D_{opt}S_o}{Y} - \frac{D_{opt}\left(\frac{D_{opt}}{a}\right)^{\frac{1}{n}}}{Y} \tag{14}$$

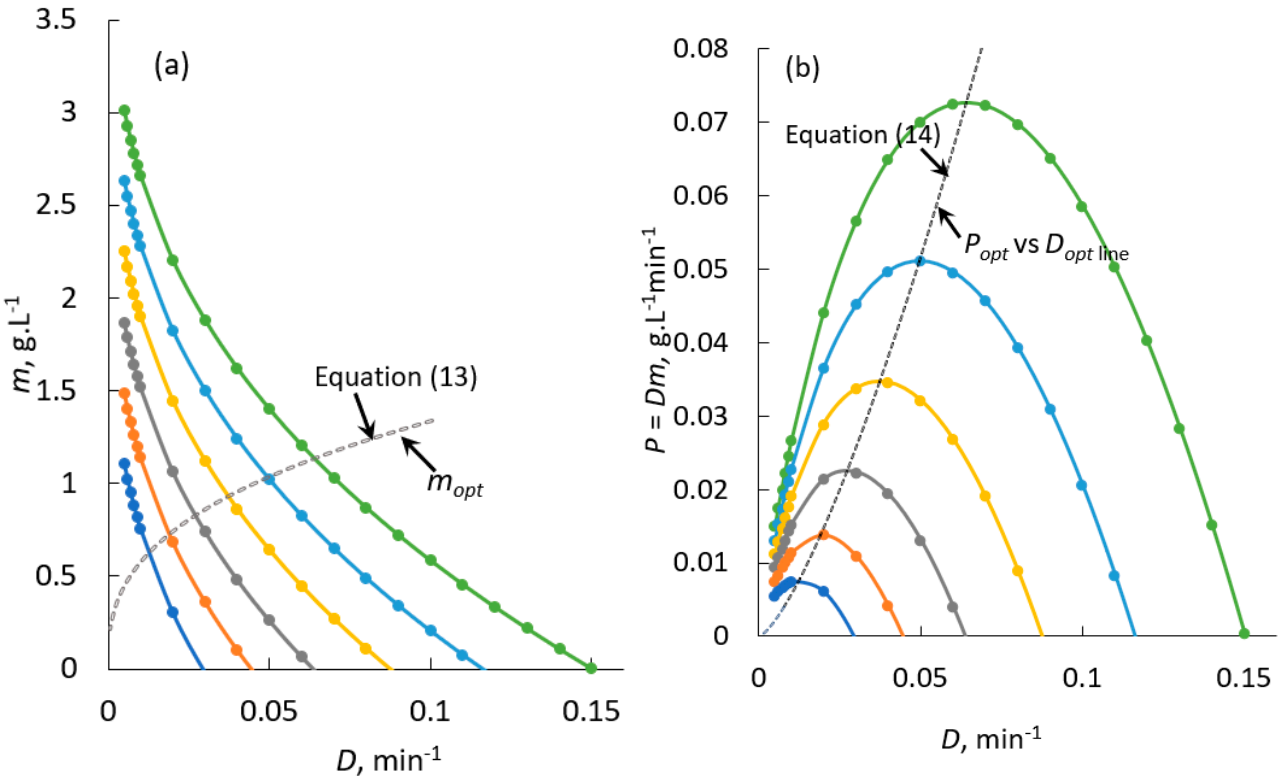


Figure 2. (**a**) plot of mass crystallised at steady state during the continuous crystallisation of curcumin in isopropanol as a function of the dilution rate (also shown is the mass crystallised when $D = D_{opt}$), (**b**) plot of productivity versus D (also shown is the productivity line when $D = D_{opt}$). (●: S_o = 3, ●: S_o = 3.5, ●: S_o = 4, ●: 4.5, ●: S_o = 5, ●: S_o = 5.5).

Both Equations (12) and (13) can be used to theoretically calculate the mass crystallised and productivity when the dilution rate $D = D_{opt}$. In Figure 2a,b, we showed the mass crystallised and the productivity at D_{opt} predicted using Equations (12) and (14), respectively. From Figure 2b, it is evident that the P_{opt} versus D_{opt} line predicted using these theoretical expressions passes through the peak maximum observed in the plot of P versus D, irrespective of the initial supersaturation. As expected, the ordinate and the abscissa of the point that correspond to the peak maximum observed in the plot of P versus D matches with P_{opt} versus D_{opt} predicted using Equations (14) and (12), respectively.

Similarly, it is possible to predict the dilution rate when the productivity reaches zero, D_{zero} (see Figure 2b). In this case, the supersaturation that exits the CSTC should be equal to the initial supersaturation. The theoretical expression can be obtained by setting P_{opt} in Equation (10) as equal to zero, and in that case the resulting dilution rate D should be equal to D_{zero}. Then, the theoretical D_{zero} is given by

$$D_{zero} = a(m_o Y + S_o)^n \quad (15)$$

Equation (15) can be used to determine the dilution rate where we will observe either washout of crystals or no secondary nucleation. In Figure 3, we show the plot of S_o versus D_{zero}. Theoretically, the D_{zero} value increases with initial supersaturation following a power-law type expression, as in Equation (15). This trend is expected because a higher supersaturation implies a greater likelihood of secondary nucleation and growth, necessitating a higher dilution rate to attain washout conditions (assuming at higher supersaturations, secondary nucleation is likely to dominate, and D_{zero} can only be achieved via washout of the crystals dictated by the high dilution rate).

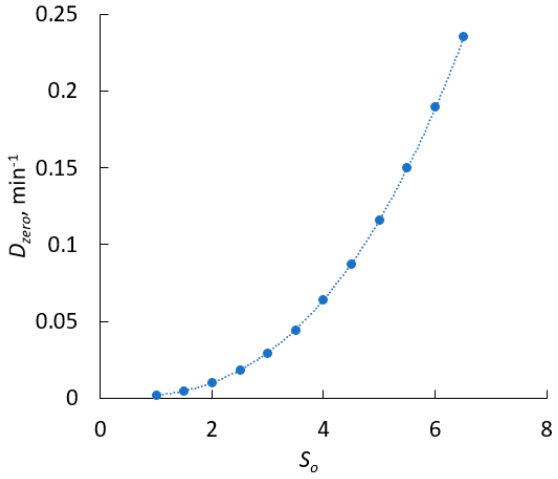


Figure 3. Plot showing the effect of initial supersaturation on the D_{zero} value.

4.3. Theoretical Procedure for the Continuous Production of Curcumin

Based on the calculated productivity and the mass crystallised at steady-state conditions, it is possible to develop theoretical procedures for the crystallisation of curcumin. In Table 1, we listed the maximum productivity, the mass crystallised when the productivity is at maximum, and the corresponding dilution rate as a function of initial supersaturation. From Table 1, it is possible to propose the operating procedure for the continuous manufacturing of curcumin for an assumed reactor volume of 100 mL. As the productivity increases with the initial supersaturation, for an assumed initial supersaturation of S_o = 5.5, we propose the following theoretical procedure for the continuous manufacturing of curcumin:

Table 1. Information required to develop a theoretical SOP for the continuous crystallisation of curcumin with solutions of different initial supersaturations.

S_o, g·L^{-1}	D_{opt}, min^{-1}	$F = V \times D$, mL·min^{-1}	V, mL	M_{opt}, g·L^{-1}	P_{max}, mg·L^{-1}min^{-1}	s,/g·L^{-1}
5.5	0.064	6.411	100	1.133	72.63	3.603
5	0.050	4.957	100	1.031	51.10	3.325
4.5	0.037	3.732	100	0.929	34.66	3.047
4	0.027	2.718	100	0.827	22.47	2.769
3.5	0.019	1.898	100	0.725	13.76	2.491
3	0.013	1.256	100	0.623	7.82	2.213
2.5	0.008	0.771	100	0.521	4.02	1.935
2	0.004	0.426	100	0.419	1.79	1.657
1.5	0.002	0.199	100	0.317	0.632	1.379
1	0.001	0.069	100	0.215	0.149	1.101

Step 1: Create the mother liquor by dissolving 4.18 g/L of curcumin in 1000 mL of solution at a temperature of 75 °C; note that this concentration is equal to the solubility concentration at 5 °C. It is best to maintain this temperature for at least 45 min to ensure complete dissolution. Step 2: For the continuous manufacturing of curcumin, it is best to operate the CSTC initially in batch mode. This means there will be no input and output streams. For this, in the crystalliser of a reactor volume of 100 mL, add 0.418 g of curcumin in 100 mL of isopropanol. Then, heat the solution to 75 °C and maintain this temperature for 45 min to ensure complete dissolution. After 45 min, cool the solution to the working temperature of 5 °C at a cooling rate of 8 K/min (this cooling rate is chosen for experimental consistency) to create supersaturation. At this temperature, the supersaturation of the solution will be at S = 5.5. Once the solution reaches the working temperature, the solution will be seeded with a known mass of curcumin crystals. Based on the experiments we performed in batch mode, we propose to add seed mass that is roughly equivalent to

1.2 wt% (a very low seed loading) of the mass crystallised to induce secondary nucleation. After secondary nucleation, wait until the solution concentration reaches the solubility concentration. Once the solution reaches saturation, the solution should now contain a solid concentration, denoted as $M = \Delta C = C_o - C^* + M_{seed}$ = (4.18 g/L−0.76 g/L + 0.042 g/L) = 3.462 g/L. At this stage, the crystalliser is set ready to change the mode of operation from batch to continuous crystallisation and will be operated as a *superstat*, and the reactor temperature will be maintained in a way so that the supersaturation inside the CSTC remains at 3–5 °C (note that at these temperatures, the S_o remains almost constant in batch reactor). Then, set the crystalliser to 3 °C before switching the mode of operation from batch to continuous mode. The temperature is purposely set to 3 °C to compensate for the expected rise in temperature in the reactor due to the mixing of the suspension in the reactor with the stream that is entering the reactor from the mother liquor tank, which is maintained at a slightly higher temperature. Step 3: Pump the mother liquor into the main crystalliser using a peristaltic pump at a flow rate of 6.41 mL·min^{-1}. As the reactor is operated in batch mode, it is also essential to set the exit stream flow rate at 6.41 mL·min^{-1} in order to maintain the reactor volume. This particular flow rate was selected based on the D_{opt} value that we determined using the theoretical expression in Equation (12); see also Figure 2b, where we show D_{opt} values as a function of initial supersaturation. Figure 2b shows that when S_o = 5.5, the D_{opt} = 0.0641 min^{-1}. The flow rate of 6.41 mL·min^{-1} divided by the reactor volume of 100 mL should give the dilution rate of 0.0641 min^{-1}, which is the D_{opt} value when S_o = 5.5. Once the flow rate of the inlet stream is set to the flow rate that corresponds to the optimum dilution rate, wait for the reactor to reach the steady state. The time to reach the steady state can be obtained by monitoring the suspension density using in situ Raman as a function of time or as a function number of residence time. Step 4: Calculation of the expected productivity and mass crystallised at steady state. According to the theoretical expression that we proposed earlier (See Equation (13) and Figure 2a), at steady state the mass crystallised or the concentration of the crystallised mass should be roughly equal to 1.133 g/L, and the productivity according to Equation (14) must be equal to 0.0726 g/L·min. If we know the initial concentration, then from the mass crystallised at steady state it is also possible to calculate the concentration of the solution in the CSTC at steady state using a simple mass balance. For S_o = 5.5, the initial concentration is given by $c = c^* \times S_o$ = 0.76 × 5.5 = 4.18 g/L. If the m_{opt} = 1.133 g/L, then the concentration of the solution at the steady state will be equal to 4.18−1.133 = 3.04 g/L. Steps 1 to 4 outlined above serve as a guideline for designing standard operating procedures (SOPs) for the continuous crystallisation of curcumin, leveraging information derived from batch kinetics. While the SOP provided assumes an initial supersaturation (So) of 5.5, it is flexible and can be adapted for other initial supersaturation values. Using the data in Table 1, it becomes straightforward to tailor an SOP for different So values. The flow rates (F) presented in Table 1 are based on a reactor volume of 100 mL, and the table also details the expected solid concentration and productivity at steady state. Crucially, all necessary information to operate a continuous stirred-tank crystalliser (CSTC) in *superstat* mode—where the feed supersaturation remains fixed and the system operates at the maximum crystallisation rate—can be derived from batch crystallisation kinetics. The kinetic constant as a function of So is key to calculating process conditions for achieving a desired theoretical productivity. The cornerstone assumption of this approach is that the CSTC operates in *superstat* mode. Once the feed supersaturation is fixed, the optimum dilution rate can be theoretically calculated using Equation (12), which relies solely on batch kinetic data. This allows for the development of a standalone protocol for continuous crystallisation. With the determined dilution rate, the mass crystallised and productivity at steady state can then be estimated using Equations (13) and (14), respectively.

5. Conclusions

To conclude, we presented the theoretical procedure to identify conditions that can be used to develop SOP for the continuous crystallisation of pharmaceuticals using the

information obtained from batch kinetics. The theoretical values that include the dilution rate, mass crystallised, productivity at steady state, optimum dilution rate, and the dilution rate that corresponds to washout conditions can be used as a preliminary step to develop a SOP for the continuous crystallisation process. The protocols discussed above only require the kinetic constant obtained from the batch crystallisation process but provide a lot of information about the required level of dilution rate for the manufacturing of pharmaceuticals in continuous mode as a function of supersaturation. For the case of continuous crystallisation of curcumin, based on the theoretical results shown in Figure 2a,b for a solution of $S_o = 5.5$, it is best to maintain a dilution rate that may range from 0.04 to 0.08 min^{-1}, and it is not advisable to operate the CSTC with $D > 0.15$ min^{-1}, where we could encounter complete washout of solid particles from the crystalliser. If we operate the crystalliser with a solution of low supersaturation, $S_o = 3$, then based on the theoretical calculations shown in Figure 2a,b, it is best to maintain the dilution rate of 0.012 min-1, where the productivity will be at maximum. In this case, we will also encounter the condition of no crystallisation or washout of crystals when the $D > 0.03$. Clearly, the proposed method can serve as a guideline for experimentalists who are developing SOP for continuous crystallisation based on the batch crystallisation kinetics. Moreover, it provides important information about expected productivity at steady-state conditions.

Author Contributions: M.V. and M.R. performed the experiments. M.V. and K.V.K. developed the theoretical model proposed in this work and wrote the first draft. M.R. also contributed to the writing of the manuscript. K.V.K. and G.W. secured the funding required for this project, provided the resources, and supervised the project. K.V.K. and G.W. also reviewed and edited the final version of the article. All authors have read and agreed to the published version of the manuscript.

Funding: The research was funded by the Science Foundation Ireland (Grant 12/RC/2275, 12/RI/2345/SOF and 18/SIRG/5479).

Data Availability Statement: The datasets generated during and/or analysed during the current study are available from the corresponding author upon reasonable request. The Excel worksheets used to perform the calculations are available upon request from the authors.

Acknowledgments: We acknowledge the financial support of Science Foundation Ireland (Grant 12/RC/2275, 12/RI/2345/SOF and 18/SIRG/5479). M.V.would like to acknowledge the Bernal Institute, Boston Scientific, Department of Chemical Sciences, and the University of Limerick Foundation for the funding support through the mULtiply program.

Conflicts of Interest: On behalf of all authors, the corresponding author states that there are no conflicts of interest.

References

1. Ginde, R.M.; Myerson, A.S. Effect of Impurities on Cluster Growth and Nucleation. *J. Cryst. Growth* **1993**, *126*, 216–222. [CrossRef]
2. Chen, J.; Sarma, B.; Evans, J.M.B.; Myerson, A.S. Pharmaceutical Crystallization. *Cryst. Growth Des.* **2011**, *11*, 887–895. [CrossRef]
3. Hsi, K.H.; Kenny, M.; Simi, A.; Myerson, A.S. Purification of Structurally Similar Compounds by the Formation of Impurity Co-Former Complexes in Solution. *Cryst. Growth Des.* **2013**, *13*, 1577–1582. [CrossRef]
4. Kuvadia, Z.B.; Doherty, M.F. Effect of Structurally Similar Additives on Crystal Habit of Organic Molecular Crystals at Low Supersaturation. *Cryst. Growth Des.* **2013**, *13*, 1412–1428. [CrossRef]
5. Mascia, S.; Heider, P.L.; Zhang, H.; Lakerveld, R.; Benyahia, B.; Barton, P.I.; Braatz, R.D.; Cooney, C.L.; Evans, J.M.B.; Jamison, T.F.; et al. End-to-End Continuous Manufacturing of Pharmaceuticals: Integrated Synthesis, Purification, and Final Dosage Formation. *Angew. Chem. Int. Ed.* **2013**, *52*, 12359–12363. [CrossRef]
6. Wood, B.; Girard, K.P.; Polster, C.S.; Croker, D.M. Progress to Date in the Design and Operation of Continuous Crystallization Processes for Pharmaceutical Applications. *Org. Process Res. Dev.* **2019**, *23*, 122–144. [CrossRef]
7. Pfizer & Siemens: Continuous Manufacturing in Pharma—YouTube. Available online: https://www.youtube.com/watch?v=AFSo8qaY5EU&t=48s (accessed on 2 August 2023).
8. Zhang, D.; Xu, S.; Du, S.; Wang, J.; Gong, J. Progress of Pharmaceutical Continuous Crystallization. *Engineering* **2017**, *3*, 354–364. [CrossRef]
9. Orehek, J.; Teslić, D.; Likozar, B. Continuous Crystallization Processes in Pharmaceutical Manufacturing: A Review. *Org. Process Res. Dev.* **2021**, *25*, 16–42. [CrossRef]

10. Wang, T.; Lu, H.; Wang, J.; Xiao, Y.; Zhou, Y.; Bao, Y.; Hao, H. Recent Progress of Continuous Crystallization. *J. Ind. Eng. Chem.* **2017**, *54*, 14–29. [CrossRef]
11. Ma, Y.; Wu, S.; Macaringue, E.G.J.; Zhang, T.; Gong, J.; Wang, J. Recent Progress in Continuous Crystallization of Pharmaceutical Products: Precise Preparation and Control. *Org. Process Res. Dev.* **2020**, *24*, 1785–1801. [CrossRef]
12. Çelik, M. Quality by Design, Process Analytical Technology, GMP and Regulatory Affairs. *Pharm. Dev. Technol.* **2018**, *23*, 553. [CrossRef] [PubMed]
13. Sontakke, G.M.; Sakhare, S.S.; Chavan, R.D.; Hamand, V.G.; Hamand, V.G. Quality Control and Quality Assurance in Pharmaceutical Industry. *Int. J. Adv. Res. Sci. Commun. Technol.* **2023**, *2*, 501–510. [CrossRef]
14. Mishra, A.K.; Singh, R.; Chaurasia, D.K.; Shukla, D.T.P. A Review: Quality Assurance and Quality Control. *Int. J. Res. Appl. Sci. Eng. Technol.* **2023**, *11*, 45. [CrossRef]
15. *Pharmaceutical Industry Wastes $50 Billion a Year Due to Inefficient Manufacturing—The Source—Washington University in St. Louis*. Available online: https://source.wustl.edu/2006/10/pharmaceutical-industry-wastes-50-billion-a-year-due-to-inefficient-manufacturing/ (accessed on 2 August 2023).
16. Center for Drug Evaluation and Research. *Q13 Continuous Manufacturing of Drug Substances and Drug Products Guidance for Industry*; Center for Drug Evaluation and Research: Silver Spring, MD, USA, 2023.
17. Domokos, A.; Nagy, B.; Gyürkés, M.; Farkas, A.; Tacsi, K.; Pataki, H.; Liu, Y.C.; Balogh, A.; Firth, P.; Szilágyi, B.; et al. End-to-End Continuous Manufacturing of Conventional Compressed Tablets: From Flow Synthesis to Tableting through Integrated Crystallization and Filtration. *Int. J. Pharm.* **2020**, *581*, 119297. [CrossRef] [PubMed]
18. Majumder, A.; Nagy, Z.K.; Ni, X.W. Recent Advances in Continuous Crystallization. *Chem. Eng. Res. Des.* **2022**, *186*, 610–613. [CrossRef]
19. Kshirsagar, S.; Szilagyi, B.; Nagy, Z.K. Experimental Design for the Efficient Determination of the Crystallization Kinetics of a Polymorphic System in Combined Cooling and Antisolvent Crystallization. *Cryst. Growth Des.* **2023**, *23*, 1486–1499. [CrossRef]
20. Nagy, Z.K.; Fujiwara, M.; Braatz, R.D. Modelling and Control of Combined Cooling and Antisolvent Crystallization Processes. *J. Process Control* **2008**, *18*, 856–864. [CrossRef]
21. Su, Q.; Nagy, Z.K.; Rielly, C.D. Pharmaceutical Crystallisation Processes from Batch to Continuous Operation Using MSMPR Stages: Modelling, Design, and Control. *Chem. Eng. Process. Process Intensif.* **2015**, *89*, 41–53. [CrossRef]
22. Li, J.; Trout, B.L.; Myerson, A.S. Multistage Continuous Mixed-Suspension, Mixed-Product Removal (MSMPR) Crystallization with Solids Recycle. *Org. Process Res. Dev.* **2016**, *20*, 510–516. [CrossRef]
23. Garslde, J.; Shah, M.B. Crystallization Kinetics from MSMPR Crystallizers. *Ind. Eng. Chem. Process Des. Dev.* **1980**, *19*, 509–514. [CrossRef]
24. Du, X.; Xie, C.; Liu, B.; Yuan, P.; Sun, H. Continuous Crystallization Process of Cefminox Sodium in MSMPR Crystallizer. *Cryst. Res. Technol.* **2023**, *58*, 2200256. [CrossRef]
25. Yazdanpanah, N.; Nagy, Z.K. *The Handbook of Continuous Crystallization*; Royal Society of Chemistry: London, UK, 2020. [CrossRef]
26. Mullin, J.W. *Crystallization*, 4th ed.; Butterworth-Heinemann: Oxford, UK, 2001; ISBN 9780750648332.
27. Som, S.; Singh, S.K.; Khatik, G.L.; Kapoor, B.; Gulati, M.; Kuppusamy, G.; Anandhakrishnan, N.K.; Kumar, B.; Yadav, A.K.; Kumar, R.; et al. Quality by Design-Based Crystallization of Curcumin Using Liquid Antisolvent Precipitation: Micromeritic, Biopharmaceutical, and Stability Aspects. *Assay Drug Dev. Technol.* **2020**, *18*, 11–33. [CrossRef] [PubMed]
28. Ukrainczyk, M.; Hodnett, B.K.; Rasmuson, Å.C. Process Parameters in the Purification of Curcumin by Cooling Crystallization. *Org. Process Res. Dev.* **2016**, *20*, 1593–1602. [CrossRef]
29. Heffernan, C.; Ukrainczyk, M.; Gamidi, R.K.; Hodnett, B.K.; Rasmuson, Å.C. Extraction and Purification of Curcuminoids from Crude Curcumin by a Combination of Crystallization and Chromatography. *Org. Process Res. Dev.* **2017**, *21*, 821–826. [CrossRef]
30. Vashistha, M.; Cliffe, C.; Murphy, E.; Palanisamy, P.; Stewart, A.; Gadipelli, S.; Howard, C.A.; Brett, D.J.L.; Kumar, K.V. Dotted Crystallisation: Nucleation Accelerated, Regulated, and Guided by Carbon Dots. *CrystEngComm* **2023**, *25*, 4729–4744. [CrossRef]
31. Kumar, K.V.; Ramisetty, K.A.; Devi, K.R.; Krishna, G.R.; Heffernan, C.; Stewart, A.A.; Guo, J.; Gadipelli, S.; Brett, D.J.L.; Favvas, E.P.; et al. Pure Curcumin Spherulites from Impure Solutions via Nonclassical Crystallization. *ACS Omega* **2021**, *6*, 23884–23900. [CrossRef]
32. Thorat, A.A.; Dalvi, S.V. Particle Formation Pathways and Polymorphism of Curcumin Induced by Ultrasound and Additives during Liquid Antisolvent Precipitation. *CrystEngComm* **2014**, *16*, 11102–11114. [CrossRef]
33. Yang, Y.; Song, L.; Gao, T.; Nagy, Z.K. Integrated Upstream and Downstream Application of Wet Milling with Continuous Mixed Suspension Mixed Product Removal Crystallization. *Cryst. Growth Des.* **2015**, *15*, 5879–5885. [CrossRef]
34. Novick, A.; Szilard, L. Description of the Chemostat. *Science* **1950**, *112*, 715–716. [CrossRef]

Disclaimer/Publisher's Note: The statements, opinions and data contained in all publications are solely those of the individual author(s) and contributor(s) and not of MDPI and/or the editor(s). MDPI and/or the editor(s) disclaim responsibility for any injury to people or property resulting from any ideas, methods, instructions or products referred to in the content.